Self-Discriminating Termination of Chiral Supramolecular Polymerization: Tuning the Length of Nanofiber**

Jatish Kumar, Hiroyuki Tsumatori, Junpei Yuasa, Tsuyoshi Kawai,* and Takuya Nakashima*

Abstract: Directing the supramolecular polymerization towards a preferred type of organization is extremely important in the design of functional soft materials. Herein, we propose a simple methodology to tune the length and optical chirality of supramolecular polymers formed from a chiral bichromophoric binaphthalene by the control of enantiomeric excess (*ee*). The enantiopure compound gave thin fibers longer than a few microns, while the racemic mixture favored the formation of particular aggregates. The thermodynamic study unveils that the heterochiral assembly gets preference over the homochiral assembly. The stronger heterochiral binding over homochiral one terminated the elongation of fibrous assembly, leading to a control over the length of fibers in nonracemic mixtures. The supramolecular polymerization driven by π-π interactions highlights the effect of the geometry of twisted π-core on this self-sorting assembly.

Past two decades have witnessed an increased attention in the field of self-assembly of small molecules into complex architectures.[1] This interest in supramolecular polymers formed *via* noncovalent interactions arises mainly due to (i) the urge to mimic the life systems by understanding the process of self-assembly in biological macromolecules[2a] and (ii) the ability to build nanostructures for practical applications utilizing a bottom-up approach.[2b-d] The bottom-up approach drives the formation of supramolecular aggregates through a combined effect of different noncovalent intermolecular forces leading to complex superstructures, often possessing fibrous nature.[3] Molecules possessing chiral centers act as building blocks for the fabrication of helical nanostructures, wherein the supramolecular chirality is determined by the chirality at the molecular level.[4,5] The fascinating structural features of different chiral nanostructures, such as helices, nanotapes and nanotubes have attracted great interest due to their resemblance to biological structures[6a] and possible applications in chiral sensing and catalysis.[6b-d]

The performance of functional organic materials in optoelectronic devices is largely dependent on the organization of molecular components.[6] Hence, directing the self-assembly towards a preferred type of organization is an extremely important step in the design of such materials. Recently, we reported the self-assembly of chiral binaphthalenes bearing two perylene bisimide (PBI) units (**1** in Scheme 1)[7] into dissimilar morphologies depending on the solvent system.[8] They formed helical fibers through π-π stacking interactions in methylcyclohexane (MCH) but spherical aggregates in chloroform at high concentration.[8] The fibrous assemblies gave superior chiroptical properties including circularly polarized luminescence (CPL) relative to the spherical aggregates. In the present work, we introduce a new methodology to control the length of the fibers through the mixing of enantiomers possessing opposite chirality. In this regard, earlier investigations have demonstrated the morphological changes of fibrous assemblies[9] with supramolecular chirality following the "majority rules" effect,[10] or the chiral self-sorting during self-organization.[11] Although most studies varying the *ee* resulted in morphological changes of fibers, to our best knowledge, no example of control on the assembly length has been reported without changing morphology. Herein, we utilize the enantiomeric mixing for controlling the length as well as the supramolecular chirality of supramolecular polymers.

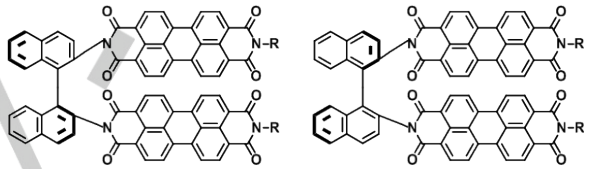

Scheme 1. Molecular structure of the *S* and *R* isomers of **1** [R = $CH(C_6H_{13})_2$].

We first examined racemic coassembly of **1**. Freshly prepared solutions of *S* and *R* isomers in chloroform:MCH (1:49) at a concentration of 1×10^{-5} M, wherein they form extended fibers,[8] were mixed at room temperature. The mixture solution was then annealed above 95 ºC, followed by slow cooling to room temperature at a rate of 1 ºC/min. The TEM image before annealing (Figure 1A) suggested that the fibers formed from enantiopure isomers remain phase separated. After annealing, the fibrous assemblies completely disappeared and ill-structured nanoparticular aggregates with a diameter of 10–20 nm were formed (Figure 1B). Similar behavior was earlier observed in the self-assemblies driven by π-π stacking interactions of core-twisted π-systems including helicene derivatives[12] and bay-substituted PBIs.[13] The injection of chloroform solutions of **1** into MCH provided similar results without annealing. The enantiopure solution gave the extended fibers while the particular aggregates were obtained by the injection of premixed-racemic chloroform solution (Figure S1). This fact indicated that annealing disassembled the aggregates into their monomeric state as dissolved in chloroform and both the fibrous and particular aggregates could be assembled from the identical monomeric state.

[*] Dr. J. Kumar, Dr. H. Tsumatori, Dr. J. Yuasa, Prof. T. Kawai, Dr. T. Nakashima
Graduate School of Materials Science, Nara Institute of Science and Technology (NAIST)
8916-5 Takayama, Ikoma, Nara 630-0192 (Japan)
E-mail: tkawai@ms.naist.jp
ntaku@ms.naist.jp

[**] The authors are most grateful to Ms. S. Fujita for the measurement of cryo-TEM. This work was supported in part by the Grand-in-Aid for Scientific Research (No. 25248019) from JSPS. JK also acknowledges JSPS for the post-doctoral fellowship.

Supporting information for this article is given via a link at the end of the document.

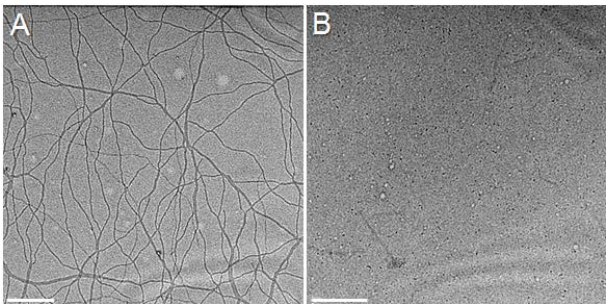

Figure 1. TEM images of racemic coassembly of *R*- and *S*-**1** (A) before and (B) after annealing at 95 ºC (scale bar = 200 nm).

The mechanistic studies on supramolecular polymerization have been well documented based on the isodesmic and cooperative models.[14] Würthner and co-workers described that the simple assemblies of PBI dyes through π-π interactions, as in our present case, were well fitted by the isodesmic model.[15] In the isodesmic model, each step of the monomer attachment to the chain-end is governed by a single equilibrium constant K_1. Temperature-dependent absorption studies showed a sigmoidal curve for the fraction of aggregates versus temperature suggesting an isodesmic model in both cases (Figure 2A). Similar fits were observed in temperature dependent CD analysis (Figure S2). A gradual disassembly profile was observed on addition of chloroform to the aggregates, confirming the isodesmic mechanism (Figure S3).[16] These studies also suggested that the racemic aggregates were more stable than the enantiopure fibers. Nonlinear least-square regression analysis of the concentration-dependent absorption spectra[15b] showed that the assembly behavior can be well described by the isodesmic model (Figure 2B) for the homochiral supramolecular polymers. The association constant at room temperature was determined as $K_{homo} = 2.0 \pm 0.1 \times 10^5\ M^{-1}$. The apparent association constant for the racemic aggregates was also roughly determined by this model to be $K_{rac} = 4.9 \pm 0.5 \times 10^5\ M^{-1}$. Since the homochiral interaction is also possible, even if it is not very likely, in the racemic solution, the practical heterochiral association constant (K_{hetero}) could be larger than K_{rac}, which apparently leads to the larger K_{hetero} than K_{homo}. In addition to the result in Figure 1, the mechanistic study indicated two important characteristics of the assemblies: (i) The enantiopure compound forms fibrous assemblies, while the racemic mixture favors the nonfibrous particular aggregates (Scheme 2), and (ii) the formation of racemic nanoparticles is thermodynamically favored over the homochiral fibers, demonstrating that self-discrimination prevails over self-recognition.

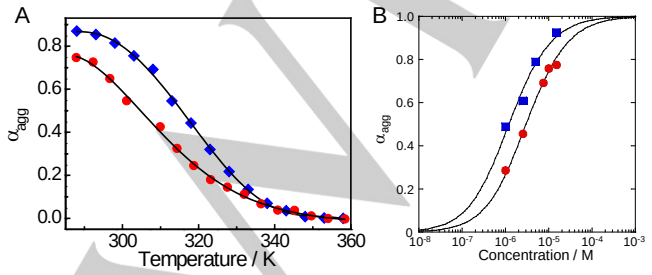

Figure 2. (A) Fraction of aggregated molecules (α_{agg}) as a function of (A) temperature and (B) total concentration of **1** in a mixture of (1:49) chloroform:MCH obtained by fitting the apparent absorption coefficients at λ = 522 nm to the isodesmic model for enantiopure (red circles) and racemic solution (blue squares). Also see Figure S4 and the footnote.

The absorption spectrum of enantiopure solution in MCH gave a profile typical to assemblies with helically arranged PBI dyes (Figure S5).[17] The intense band at 550 nm in the enantiopure solution shifted to 545 nm with emergence of a shoulder at 565 nm in the racemic one, indicating a change in packing arrangement. The rough conformational searches of dimeric models with the MMFF94s force field using the CONFLEX program[18] gave dissimilar structures (Figure S6). The heterochiral dimer showed a complementary stack, while the optimized homochiral dimer had rotationally displaced PBI units (Scheme 2). The heterodimer gave the smaller steric energy than that of homodimer.

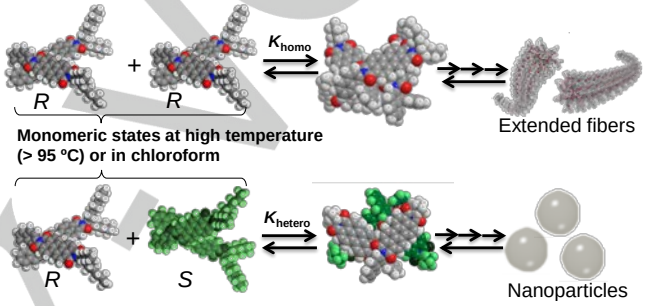

Scheme 2. Schematic illustration of assembly of **1** in homochiral and racemic systems together with dimeric models calculated by MMFFs94.

The stronger heterochiral interaction over homochiral one inspired us to control the length of fibers by varying *ee* through the self-sorting property in the supramolecular polymerization. The fibrous growth *via* the self-recognition with K_{homo} could be deactivated by the heterochiral interactions which prefer nonfibrous growth. The elongation and deactivation of fibrous growth at the ends are thermodynamically controlled with K_{homo} and K_{hetero}, respectively. Meanwhile, the probabilities of homochiral and heterochiral interactions should be stochastically controlled by *ee*, which would lead to the controlled persistent homochiral growth of fibers. The length of supramolecular polymers is usually controlled by varying temperature, concentration and solvent-composition.[14a] In this context, recently Takeuchi, Sugiyasu and coworkers have succeeded in controlling the length of supramolecular polymers based on porphyrin assemblies with a narrow polydispersity.[19] They employed an interplay of isodesmic and cooperative aggregation pathways to achieve living supramolecular polymerization. The present study is the first attempt to control the length of supramolecular fibers in terms of *ee*, or through an interplay of chiral self-recognition and self-discrimination behaviors.

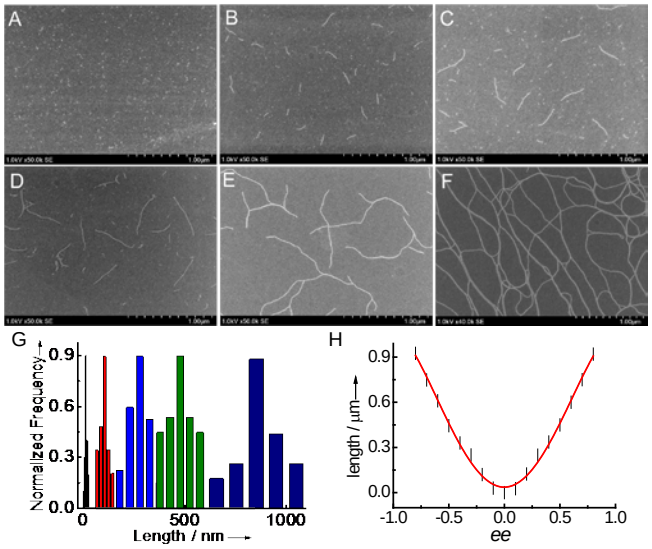

Figure 3. SEM images of coassembly of *R*- and *S*-**1** at *ee* (a) 0.0, (B) 0.2, (C) 0.4, (D) 0.6, (E) 0.8 and (F) 1.0. (G) Histogram of the length distribution of nanofibers obtained by measuring 50 fibers for ee 0.0 (black), 0.2 (red), 0.4 (blue), 0.6 (green) and 0.8 (navy blue). (H) A plot of average length of nanofibers versus the *ee*.

The coassemblies of *S*- and *R*-**1** with different *ee* values were characterized by SEM (Figures 3 and S7, also see Figures S8, S9 and S10 for TEM, AFM, and cryo-TEM images, respectively). Very interestingly, the self-assembly at different *ee* resulted in fibrous structures with varying lengths without changing the morphology and the width of fibers. The enantiopure assembly resulted in extended fibers longer than a few microns with width of 9 ± 3 nm after accounting for the AFM tip-broadening factor. The line profile analysis of topographic image obtained by AFM estimated the height of fibers to be about 4 ± 0.5 nm, almost corresponding to a unimolecular length. The length of the fibers decreased with decreasing *ee*, leading to the formation of particles possessing an average diameter of 10–20 nm for the racemic mixture. At higher *ee* of 0.8 and 0.9, the nanostructures are composed of longer fibers along with shorter fibers. For *ee* between 0.8 and 0.2, only shorter fibers could be observed, the length of which was sharply dependent on the *ee*. Histogram of the length distribution of the fibrous structures obtained by measuring 50 fibers shows clear increase in the length of fibers with increasing *ee* (Figure 2G). An average length of ~125±20, ~275±35 and ~490±50 nm was observed for fibers with *ee* of 0.2, 0.4 and 0.6, respectively (Figures 2B, C, D). A plot of the size of nanofibers versus the *ee* gives a parabolic curve suggesting a precise control over the length by varying *ee* (Figure 2H). It should be noted that the cryo-TEM images directly demonstrated that the length of fibrous assemblies was indeed controlled in the solution state.

Meanwhile, the nanoparticles coexisted for the samples with *ee* below 0.6. One may wonder if the racemic portion provided nanoparticles and the remaining enantiopure component self-assembled into short fibers. However, under this assumption, the length of fiber should depend on the concentration of enantiopure molecule. On the other hand, the extended fibers were formed regardless of the concentration (Figure S11 and S12), clearly disproving this assumption. It also appears that a single heterochiral binding does not always terminate the fibrous growth completely. That is, for example, even the mixture of *ee* = 0.9, in which no particles coexisted in a SEM image, contains a 5% portion of minor enantiomer, wherein the average number of enantiomer in an uninterrupted homochiral sequence could be only 10.5 under a random copolymerization condition.[20] This number seems far small considering the length of fibers observed. The relatively small difference between K_{homo} and K_{hetero} with a similar order of magnitude may tolerate the incorporation of opposite enantiomer in the fibers. Taking above discussion into account, there are three possibilities for minor enantiomer in nonracemic mixtures; to form racemic particles (*ee* < 0.6), be incorporated in the fibers with a nonpreferred screw sense at the cost of mismatch penalty,[21] and terminate the fibrous growth at the ends. Therefore, a certain number of successive heterochial interactions at the growing end may be necessary to terminate the supramolecular polymerization.

We then investigated the change of optical chirality with varying *ee*. In absorption spectra, a gradual hypsochromic shift in peak positions accompanying a slight hypochromic effect was observed with decrease in *ee* (Figure S5). This result also rules out the possibility of the phase separation between racemic particles and enantiopure fibers for the samples with *ee* < 0.6 but suggests the change in the molecular packing. The self-assembly of the pure components resulted in mirror image CD profiles with the negative and positive first Cotton effects for the *R* and *S* isomers, respectively, which originate from the supramolecular excitonic interactions in chiral assemblies (Figure 3A).[8] Interestingly, with a decrease in enantiomeric ratio a gradual decrease in the CD intensity of peak at 564 nm was observed with the formation of a new band at 546 nm. The CD intensity of this new band for *ee* of 0.4 was larger than that for *ee* of 0.6, which indicated a substantial shift in components and molecular ordering responsible for the supramolecular exciton coupling in the self-assemblies. The aforementioned erratic incorporation of the opposite enantiomers in the fibers with a nonpreferred screw sense could lead to the change in the chiral packing mode and the consequent supramolecular chirality. The distinctive chiral bichromophoric geometry in a monomeric component could disrupt the helical arrangement of PBIs when incorporated in a fiber with a nonpreferred screw sense. This effect could cause the more complex CD response with a peak shift than other monochromophoric systems complying with the "majority rules" effect.[14a,21] The maximum value of dissymmetry factor (g_{CD}) $\Delta\varepsilon/\varepsilon$ plotted against the *ee* deviates from linearity, suggesting that a certain amount of "majority rules" effect was displayed (Figure 4C). For the samples without annealing, a linear fit for the g_{CD} versus *ee* plot were observed, which is indicative of the fact that the long fibers formed from *S* and *R* isomers remain phase separated before annealing (Figure S13). That is, the CD intensity at each *ee* is expressed as the sum of opposite contributions of chiral fibers composed of pure enantiomers.

A gradual quenching in fluorescence peak at 630 nm, corresponding to emission from assemblies was observed with decreasing *ee* (Figure S5). Fluorescence quantum yield decreased from a value of 0.45 for *ee* of 1.0 to 0.24 for *ee* of 0.0 (Table S1) and a plot of quantum yield against *ee* showed sigmoidal fit similar to the CD result (Figure S14). The molecular ordering for the efficient energy migration is most likely to be disturbed by the heterochiral interactions in the assemblies.[13,22] The CPL spectra exhibited peaks at the corresponding fluorescence wavelengths, the intensity of which decreased with decreasing *ee* (Figure 4B). The helical fibers of pure components exhibited relatively high CPL activity with g_{lum} value of 0.02.[8] The sum of cooperative excitonic couplings between the individual components resulted in remarkably high value of fluorescence dissymmetry for the aggregated structures.[8,22] Similar to the results obtained in the CD profile, a plot of

g_{lum} against *ee* exhibited a sigmoidal relationship (Figure 4D). This plot demonstrates a new methodology for the design of self-assembled nanosystems with desired luminescence dissymmetry.

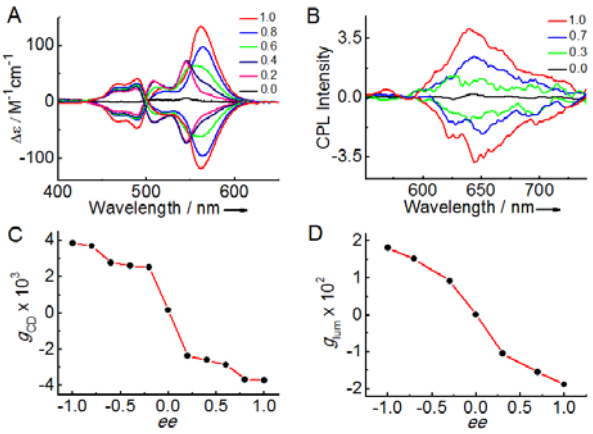

Figure 4. (a) CD and (b) CPL spectra of coassembly of *R*- and *S*-**1** at varying *ee*. (E) Plot of maximum g_{CD} versus *ee* and (F) g_{lum} at 640 nm plotted against the *ee*.

We thus could demonstrate that the length of the fibrous structures as well as their supramolecular chirality were sharply dependent on the *ee*. The successful control could be attributed to the molecular design of **1**, which favors the isodesmic supramolecualr polymerization controlled simply by K_{homo} and K_{hetero} based on the π-π stacking of the twisted cores. The geometry, or the direction of twisting of the core dictated by the axial chirality of binaphthalene unit, therefore, is critical for the growth of assembly through the stacking of cores, which leads to the effective chiral self-sorting.[13] The similar effect of the geometries of twisted π-cores was demonstrated by the self-sorting behavior in the dimerization of bay-substituted PBIs,[23] whereas the bichromophoric system is expected to highlight this effect in the present system. The additional introduction of hydrogen bonding interaction substantially stronger than π-π interaction may increase the introduction of opposite enantiomers, which often results in the morphological change of aggregated structures as exemplified in many cases.[9,12]

In conclusion, we have demonstrated the control of the length of supramolecular polymers as well as chiroptical properties of a bichromophoric binaphthalene derivative by varying the *ee*. The key features of the present system for successfully controlling the length of supramolecular polymers include the following points. (i) The homochiral binding favors the fibrous growth whereas the heterochiral association leads to the nonfibrous assembly and both events take place under the isodesmic condition simply controlled by K_{homo} and K_{hetero}, respectively. (ii) The binding constant for the nonfibrous assembly should be larger than that for the fibrous assembly. (iii) The absence of the hydrogen bonding interaction emphasizes the effects of geometry of the twisting bichromophoric π-core in self-assembling processes, leading to an efficient self-sorting behavior. The homochiral assembly *via* self-recognition enabled the fibrous growth, which was efficiently terminated by the heterochiral bindings through the self-discrimination. Although the polydispersity cannot be well-controlled through the isodesmic system,[24] these findings still add a new guiding principle for the control of supramolecular polymerization.[14a]

Keywords: self-assembly • supramolecular chemistry • enantomeric excess • perylene dyes •circularly polarized luminescence

[1] a) S. J. Rowan, S. J. Cantrill, G. R. L. Cousins, J. K. M. Sanders, J. F. Stoddart, *Angew. Chem. Int. Ed.* **2002**, *41*, 898–952; b) M. Figueira-Duarte, K. Müllen, *Chem. Rev.* **2011**, *111*, 7260–7314; c)S. S. Babu, V. K. Praveen, A. Ajayaghosh, *Chem. Rev.*, **2014**, *114*, 1973–2129.

[2] a) D. A. Uhlenheuer, K. Petkau, L. Brunsveld, *Chem. Soc. Rev.* **2010**, *39*, 2817–2826; b) S. S. Babu, S. Prasanthkumar, A. Ajayaghosh, *Angew. Chem. Int. Ed.* **2012**, *51*, 1766–1776; c) F. Würthner, K. Meerholz, *Chem. Eur. J.* **2010**, *16*, 9366–9373; d) M. R. Wasielewski, *Acc. Chem. Res.* **2009**, *42*, 1910–1921.

[3] a) R. S. Johnson, T. Yamazaki, A. Kovalenko, H. Fenniri, *J. Am. Chem. Soc.* **2007**, *129*, 5735−5743; b) J. M. Lim, P. Kim, M. -C. Yoon, J. Sung, V. Dehm, Z. Chen, F. Würthner, D. Kim, *Chem. Sci.* **2013**, *4*, 388−397.

[4] a) M. B. Avinash, T. Govindaraju, *Adv. Mater.* **2012**, *24*, 3905–3922; b) K. Sugiyasu, N. Fujita, S. Shinkai, *Angew. Chem. Int. Ed.* **2004**, *43*, 1229–1233; c) L. Zhang, L. Qin, X. Wang, H. Cao, M. Liu, *Adv. Mater.*, **2014**, 26, 6959–6964; d) Y. Yang, Y. Zhang, Z. Wei, *Adv. Mater.* **2013**, *25*, 6039–6049.

[5] a) S. Yagai, S. Mahesh, Y. Kikkawa, K. Unoike, T. Karatsu, A. Kitamura, A. Ajayaghosh, *Angew. Chem., Int. Ed.* **2008**, *47*, 4691−4694; b) J. Kumar, T. Nakashima, T. Kawai, *Langmuir* **2014**, *30*, 6030−6037.

[6] a) C. F. Lopez, S. O. Nielsen, P. B. Moore, M. L. Klein, *Proc. Natl. Acad. Sci. USA* **2004**, *101*, 4431–4434; b) J. Hu, W. Kuang, K. Deng, W. Zou, Y. Huang, Z. Wei, C. F.J. Faul, *Adv. Funct. Mater.* **2012**, *22*, 4149–4158; c) H. Peng, L. Ding, T. Liu, X. Chen, L. Li, S. Yin, Y. Fang, *Chem. Asian J.* **2012**, *7*, 1576–1582; d) N. Mizoshita, T. Tani, S. Inagaki, *Adv. Mater.* **2012**, *24*, 3350–3355.

[7] a) H. Langhals, A. Hofer, S. Bernhard, J. S. Siegel, P. Mayer, *J. Org. Chem.* **2011**, *76*, 990−992; b) H. Langhals, *Helv. Chim. Acta* **2005**, *88*, 1309−1343; c) T. Kawai, K. Kawamura, H. Tsumatori, M. Ishikawa, M. Naito, M. Fujiki, T. Nakashima, *ChemPhysChem* **2007**, *8*, 1465-1468; d) H. Tsumatori, T. Nakashima, T. Kawai, *Org. Lett.* **2010**, *12*, 2362−2365.

[8] J. Kumar, T. Nakashima, H. Tsumatori, T. Kawai, *J Phys. Chem. Lett.* **2014**, *5*, 316−325.

[9] a) R. Oda, I. Huc, M. Schmutz, S. J. Candau, F. C. MacKintosh, *Nature* **1999**, *399*, 566−569; b) D. Berthier, T. Buffeteau, J.-M. Leger, R. Oda, I. Huc, *J. Am. Chem. Soc.* **2002**, *124*, 13486–13494; c) X. Zhu, Y. Li, P. Duan, M. Liu, *Chem. Eur. J.* **2010**, *16*, 8034–8040; d) H. Cao, X. Zhu, M. Liu, *Angew. Chem. Int. Ed.* **2013**, *52*, 4122–4126.

[10] a) W. Jin, T. Fukushima, M. Niki, A. Kosaka, N. Ishii, T. Aida, *Proc. Natl. Acad. Sci. USA* **2005**, *102*, 10801–10806; b) A. Lohr, F. Würthner, *Angew. Chem. Int. Ed. 47*, 1232-1236; c) M. M. J. Smulders, I. A. W. Filot, J. M. A. Leenders, P. van der Schoot, A. R. A. Palmans, A. P. H. J. Schenning, E. W. Meijer, *J. Am. Chem. Soc.* **2010**, *132*, 611–619; d) M. M. J. Smulders, P. J. M. Stals, T. Mes, T. F. E. Paffen, A. P. H. J. Schenning, A. R. A. Palmans, E. W. Meijer, *J. Am. Chem. Soc.* **2010**, *132*, 620–626.

[11] a) K. Sato, Y. Itoh, T. Aida, *Chem. Sci.*, **2014**, *5*, 136–140; b) C. Roche, H. J. Sun, M. E. Prendergast, P. Leowanawat, B. E. Partridge, P. A. Heiney, F. Araoka, R. Graf, H. W. Spiess, X. Zeng, G. Ungar, V. Percec, *J. Am. Chem. Soc.* **2014**, *136*, 7169-7185..

[12] T. Kaseyama, S. Furumi, X. Zhang, K. Tanaka, M. Takeuchi, *Angew. Chem. Int. Ed.* **2011**, *50*, 3684–3687.

[13] Z. Xie, V. Stepanenko, K. Radacki, F. Würthner,*Chem. Eur. J.* **2012**, *18*, 7060–7070

[14] a) T. F. A. D. Greef, M. M. J. Smulders, M. Wolffs, A. P. H. J. Schenning, R. P. Sijbesma, E. W. Meijer, *Chem. Rev.* **2009**, *109*, 5687–5754; b) C. Kulkarni, S. Balasubramanian, S. J. George, *ChemPhysChem* **2013**, *14*, 661–673.

[15] a) Z. Chen, V. Stepanenko, V. Dehm, P. Prins, L. D. A. Siebbeles, J. Seibt, P. Marquetand, V. Engel, F. Würthner, *Chem. Eur. J.* **2007**, *13*, 436–449; b) T. E. Kaiser, V. Stepanenko, F. Würthner, *J. Am. Chem. Soc.* **2009**, *131*, 6719–6732.

[16] P. A. Korevaar, C. Schaefer, T. F. A. D. Greef, E. W. Meijer, *J. Am. Chem. Soc.* **2012**, *134*, 13482−13491.

[17] J. M. Lim, P. Kim, M. C. Yoon, J. Sung, V. Dehm, Z. J. Chen, F. Würthner, D. Kim, *Chem. Sci.* **2013**, *4*, 388–397.

[18] H. Goto, E. Osawa, *J. Am. Chem. Soc.* **1989**, *111*, 8950–8951.

[19] a) S. Ogi, K. Sugiyasu, S. Manna, S. Samitsu, M. Takeuchi, *Nat. Chem.* **2014**, *6*, 188–195; b) S. Ogi, T. Fukui, M. L. Jue, M. Takeuchi, K. Sugiyasu, *Angew. Chem. Int. Ed.* **2014**, *53*, 14363–14367.

[20] H. J. Harwood, *Angew. Chem. Int. Ed.* **1965**, *4*, 394-401.

[21] a) J. van Gestel, A. R. Palmans, B. Titulaer, J. A. Vekemans, E. W. Meijer, *J. Am. Chem. Soc.* **2005**, *127*, 5490-5494; b) H. M. ten Eikelder, A. J. Markvoort, T. F. de Greef, P. A. Hilbers, *J. Phys. Chem. B* **2012**, *116*, 5291-5301.

[22] J. Kumar, T. Nakashima, H. Tsumatori, M. Mori, M. Naito, T. Kawai, *Chem. Eur. J.* **2013**, *19*, 14090−14097.

[23] M. M. Safont-Sempere, P. Osswald, M. Stolte, M. Grune, M. Renz, M. Kaupp, K. Radacki, H. Braunschweig, F. Würthner, *J. Am. Chem. Soc.* **2011**, *133*, 9580-9591.

[24] S. A. Schmid, R. Abbel, A. P. Schenning, E. W. Meijer, R. P. Sijbesma, L. M. Herz, *J. Am. Chem. Soc.* **2009**, *131*, 17696-17704.

Entry for the Table of Contents

COMMUNICATION

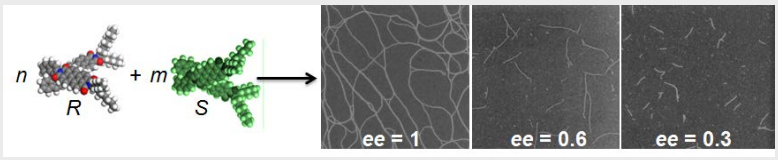

The length of chiral supramolecular polymers was precisely controlled through varying the enantiomeric excess. The homochiral assembly favors the fibrous growth whereas the heterochiral one preferentially leads to particular aggregates. The stronger heterochiral bindings at the growing ends of fibers effectively terminate the elongation of the fibers.

Jatish Kumar, Hiroyuki Tsumatori, Junpei Yuasa, Tsuyoshi Kawai, and Takuya Nakashima**

Page No. – Page No.

Self-Discriminating Termination of Chiral Supramolecular Polymerization: Tuning the Length of Nanofiber